sciendo

POLISH MARITIME RESEARCH 1 (117) 2023 Vol. 30; pp. 33-42
10.2478/pomr-2023-0004

THREE-DIMENSIONAL UNDERWATER PATH PLANNING BASED ON MODIFIED POTENTIAL FIELD ALGORITHM IN TIME-VARYING CURRENT

Shasha Wang [1]
Guilin Feng [2]
Dan Wang [1]
Yulong Tuo* [1]
[1] College of Marine Electrical Engineering, Dalian Maritime University, Dalian, China
[2] Qingdao Special Equipment Inspection Research Institute, Qingdao, China

* Corresponding author: *tuoyulong@dlmu.edu.cn(Yulong Tuo)*

ABSTRACT

The article addresses the three-dimensional (3D) underwater path planning problem of an autonomous underwater vehicle (AUV) in a time-varying current. A modified artificial potential field algorithm combining the velocity vector synthesis method is proposed to search for the optimal path. The modified potential field (MPF) algorithm is designed to dynamically plan the non-collision path. Meanwhile, this modified method is also proved to be an effective solution to the goals not reachable with obstacles nearby (GNRON), U-shaped trap, and rotation unreachable problems. To offset the influence of time-varying current, the velocity synthesis approach is designed to adjust the AUV movement direction. Besides, considering path planning in the complex underwater environment, the multi-beam forward-looking sonar (FLS) model is used. Finally, simulation studies substantiate that the designed algorithm can implement the AUV path planning effectively and successfully in a 3D underwater environment.

Keywords: AUV, 3D underwater path planning, time-varying current, modified artificial potential field, velocity synthesis

INTRODUCTION

Autonomous underwater vehicles (AUVs) are used to perform various tasks [1], such as measuring ocean parameters and monitoring, oceanography surveys, and security and acoustic surveillance. The AUVs have lower operating costs than those of manned vehicles especially when working for a long time underwater [2]-[4]. Three-dimensional (3D) path planning is an essential precondition and requirement for the intelligence and autonomy of AUVs in underwater missions, such as cooperative tracking, flocking, hunting and pursuit-evasion [5]-[7]. It is a process in which the AUV finds a path from the initial or current position to its destination according to some criteria of safety, mobility, and optimality [8]-[11]. Specifically, obstacles are inevitable in the complex underwater environment. Therefore, obstacle avoidance must be considered for the 3D path planning of AUVs.

In recent years, many approaches have been presented and used for the AUV path planning problem, which include the A* method [12], field D* method [13], Dijkstra's method [14], rapid exploration random tree (RRT) [15][16], the fast marching (FM) method [17][18] and artificial potential field (APF) [19]. Potential field methods have rapidly gained increased popularity in obstacle avoidance applications for autonomous vehicles and robots, owing to their elegance and mathematical simplicity [20]-[22]. Meanwhile, they have some inherent limitations. Perhaps the most often-mentioned problem with potential field methods (PFMs) is the trapping or local minima cases. When the AUV enters a dead end (such as a U-shaped obstacle), a trapping situation may occur. Besides, the goals not reachable with obstacles nearby (GNRON) problem may occur in cases where the goal position is quite close to an obstacle [21]. Among them, when the AUV approaches the target, it will also near the

obstacle. If the repulsive and attractive potentials are defined as common forms, the attractive force will be much smaller than the repulsive force, and the goal position is not the global minimum of the total potential. So, the AUV cannot reach its target due to the obstacle nearby.

For the above issue of APFs, researchers have proposed many effective solutions, mainly including two kinds. The first method is to improve the potential field function to eliminate the local minimum point, and ensure that the destination point is the minimum point of the global potential field to reduce the probability of local minimum points in the potential field [23][24]. The second one is combined with the APF method and other methods, so that the autonomous vehicle or robot can escape from the local minimum position [25]-[27]. The heterogeneous-ants-based path planner was proposed as a global path planner to directly find a smoother and optimal path [28]. The deep deterministic policy gradient algorithm is combined with the APF method to solve the safe navigation problem for AUV in the two-dimensional (2D) underwater environment [29]. However, to the best of our knowledge, the combination methods will increase the computational complexity, and affect the real-time performance of the APF.

Moreover, the underwater environment is a complex, uncertain, and unstable space. Most of the above studies focused on generating valid paths, and ignored the impact of other environmental factors (such as current), which is unreasonable [30][31]. In particular, the current change has a great influence on AUV navigation. Thence, the design of the AUV path planning algorithm should consider environmental factors. Meanwhile, to reduce the memory requirement and speed up the planning process, most of the above-mentioned methods in the literature have been tested and applied in a 2D environment. But in the complex underwater environment, the practical AUV motion needs to follow a 3D route [32]-[34]. Compared to the simple 2D path, a 3D route is more practical but difficult, since the path has to be generated and modified in real time to improve the AUV's adaptability to complex environments. In [31], a biologically inspired neural dynamics method based on map planning is proposed for obstacle avoidance of an AUV in a 2D non-stationary environment. In [35], an optimized fuzzy control algorithm combined with particle swarm optimization (PSO) is proposed for AUV path planning to generate an optimal 3D path. The disadvantage is that it ignores the influence of time-varying ocean currents. However, these studies only studied the constant current and path planning limits (with limited distance from obstacles) applicable to the AUV platform. For 3D AUV navigation, time-varying current should be considered.

Inspired by [30]-[35], to solve the 3D path planning problem for an AUV in an underwater environment, this article proposes an MPF-based velocity synthesis (VS) algorithm to plan the non-collision path under the influence of time-varying current, as shown in Fig. 1. The underwater environment model is constructed through multi-beam FLS. The main advantages of this article include:

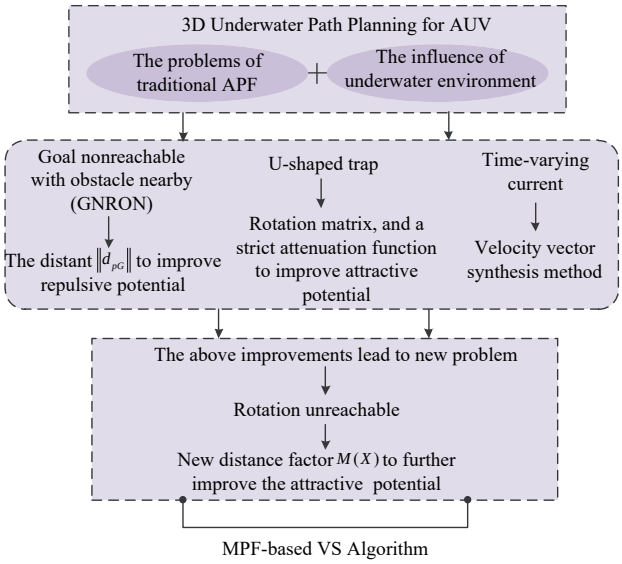

Fig. 1. 3D underwater path planning for AUV

1) Unlike the traditional APF schemes in [20]-[22], the proposed MPF method is designed to solve the GNRON and U-shaped trap problems. Besides, the attractive potential is modified to solve the new problem of rotation unreachable (a special case of GNRON and U-shaped trap).
2) Unlike existing path planning methods in [31][35], a method that combines MPF with VS is proposed to enhance the robustness of the AUV path planner in time-varying current.
3) In contrast to the methods in [30][31], the proposed algorithm is more versatile since the path planning module is suitable for a 3D underwater environment.

The organization of this article is as follows. The problem statement is presented in Section 2. Section 3 describes the proposed MPF-based VS algorithm for 3D underwater path planning of the AUV. Section 4 gives the simulations to certify the performance of the proposed algorithm. The summary and further work are presented in Section 5.

PROBLEM STATEMENT

Consider the mathematical models for an AUV, shown in Fig. 2. The simplified kinematic model (four degrees of freedom) can be defined as [35]-[37]

$$\dot{\eta} = \begin{bmatrix} \dot{x} & \dot{y} & \dot{z} & \dot{\theta} & \dot{\psi} \end{bmatrix}^T = J(\eta)v = \begin{bmatrix} \cos\psi\cos\theta & \cos\psi\sin\theta & 0 & 0 \\ \sin\psi\cos\theta & \sin\psi\sin\theta & 0 & 0 \\ -\sin\theta & \cos\psi & 0 & 0 \\ 0 & 0 & 1 & 0 \\ 0 & 0 & 0 & \frac{1}{\cos\theta} \end{bmatrix} \begin{bmatrix} u \\ w \\ q \\ r \end{bmatrix} \quad (1)$$

where η is the AUV position and orientation state vector in the earth-fixed frame. $v = [u\ w\ q\ t]^{\mathrm{T}}$ is the velocity state vector in the body-fixed frame. Variables u and w are surge and heave velocities. q and r are the pitch velocity and yaw

velocity, respectively. x, y, z are the displacement coordinates. The variable θ denotes the orientation angle and ψ is the heading angle.

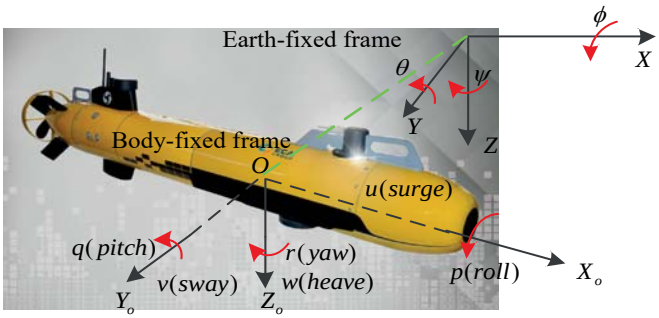

Fig. 2. AUV coordinate systems

As the AUV works in a 3D underwater environment, information needs to be gathered from its surroundings by a multi-beam forward-looking sonar (FLS) [38]. Fig. 3 shows the main parameters of the sensor. The sonar can detect obstacles in its vision, calculate the coordinates of the intersection of the surface of the obstacle and 240 beam rays, and calculate the distance between the sonar head and the intersection.

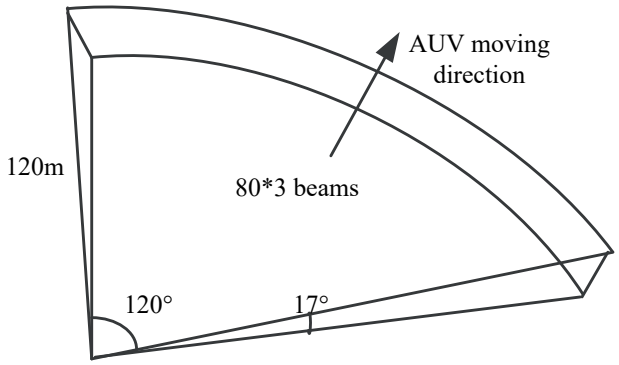

Fig. 3. The main parameters of multi-beam FLS

According to the actual situation, the 3D underwater environment includes obstacles and timevarying current, as shown in Fig. 4. Thus, the APF approach is to establish an attractive potential field function (U_{rep}) and repulsive potential field function (U_{att}) around the goal point and the obstacles, respectively. The total potential field function (U_{total}) is the superposition of the two potential fields, which determines the motion for the AUV (shown in Fig. 4). Moreover, the motion is considered in 3D space; the initial position of the AUV is $X = [x, y, z]^T$; the target position is $G = [x_{goal}, y_{goal}, z_{goal}]^T$, and the obstacle position is $O = [x_o, y_o, z_o]^T$. The potential field forces as follows are three-dimensional forced vectors.

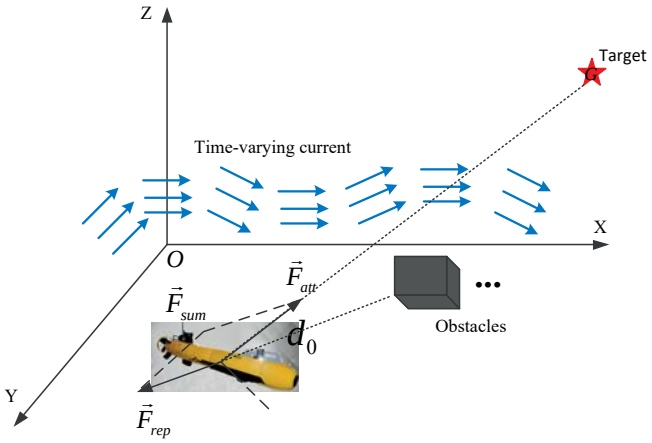

Fig. 4. 3D underwater path planning problem

In the 3D path, the potential functions for the APF are described as follows [30]:

$$U_{total}(X) = U_{att}(X) + U_{rep}(X) \tag{2}$$

$$U_{att}(X) = \frac{1}{2}\lambda_1 \|d_{XG}\|^2 \tag{3}$$

$$U_{rep}(X) = \begin{cases} \frac{1}{2}\lambda_2 \left(\frac{1}{\|d_{XO}\|} - \frac{1}{\|d_o\|}\right)^2 & \|d_{XO}\| < d_o \\ 0 & \|d_{XO}\| \geq d_o \end{cases} \tag{4}$$

where λ_1, λ_2 (λ>0) are the attractive and repulsive proportional gains of the functions. $d_{XG} = \|G_{goal} - X\|$ expresses the distance between the target and the AUV. $\|d_o\|$ represents the limit distance of the influence of the potential field, and $\|d_{XO}\|$ is the shortest distance to the obstacle and the AUV. The distance is dependent on Euclidean distances and vector algebra, the same as in the 2D environment.

The corresponding force is the negative gradient of potential, and the AUV navigates using the force given by

$$\begin{cases} \vec{F}_{att}(X) = -\nabla U_{att}(X) \\ \vec{F}_{rep}(X) = -\nabla U_{rep}(X) \\ \vec{F}_{total}(X) = \vec{F}_{rep}(X) + \vec{F}_{att}(X) \\ \qquad\qquad = -\nabla U_{total}(X) \end{cases} \tag{5}$$

The traditional APF method cannot guarantee that the AUV reaches the target position in many cases. The aforementioned literature reports some of the limitations of this method [20]-[22]. At the same time, the following assumptions are given:

Assumption 1: Complicated obstacles can be decomposed into simplified models, such as cuboids, floating balls, U-shaped, and so on. They can be superimposed on each other, the main parameters of which are geometric centroid, radius and $\|d_o\|$.

Assumption 2: The distances of obstacles, targets and AUVs refer to the distances of their geometric centroids. And their own radii also need to be considered for collision avoidance.

Assumption 3: The convergence distance Δd is set as 0.02 m, and defined as the acceptable distance range from the target point coordinates to the AUV position.

PROPOSED APPROACH

In this section, an MPF-based velocity synthesis approach to 3D underwater path planning of an AUV is proposed with static obstacles and time-varying current. Here, the MPF is used for path planning to guide AUVs to avoid obstacles.

A. Velocity vector synthesis method

The basic idea of the VS algorithm is to control the movement direction of the AUV, offset the influence of the current on the AUV navigation, and make the resultant vector point to the destination. It is shown in Fig. 5,

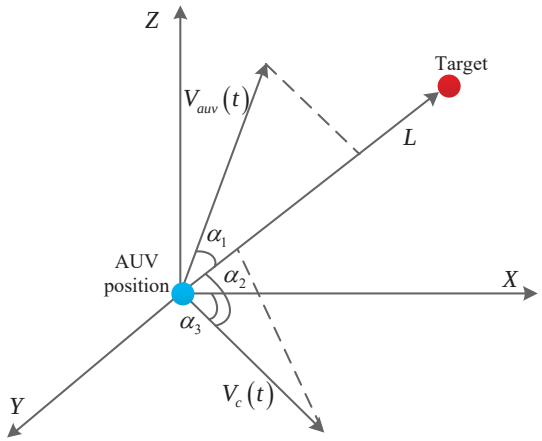

Fig. 5. Algorithm of the velocity vector synthesis

where L is the vector from the initial position of the AUV to the target. The vector $V_{auv}(t)$ is the moving speed of the AUV, and $|V_{auv}(t)|$ is known. $V_c(t)$ is the velocity of the time-varying current. α_1 represents the angle between $V_{auv}(t)$ and L. α_2 is the angle between the positive direction of $V_c(t)$ and L, and α_3 is the angle between the positive direction of the x-axis and $V_c(t)$.

In order to make the resultant velocity vector of the AUV velocity and the ocean current velocity point to L, first, the vectors $V_{auv}(t)$ and $V_c(t)$ are decomposed, and the component perpendicular to L is denoted as $V_{auvd}(t)$ and $V_{cd}(t)$, such that

$$\begin{cases} |V_{auvd}(t)| = |V_{auv}(t)| \sin\alpha_1 \\ |V_{cd}(t)| = |V_c(t)| \sin(\alpha_2 + \alpha_3) \end{cases} \quad (6)$$

Then, the AUV velocity component is made to offset the ocean current velocity component, namely

$$|V_{auv}(t)| \sin\alpha_1 = |V_c(t)| \sin(\alpha_2 + \alpha_3) \quad (7)$$

B. MPF-based velocity synthesis algorithm

The MPF-based velocity synthesis algorithm uses the goal, obstacle, and AUV positions as features to obtain a sequence of objective points that the AUV must attain, and gradient information influenced by the attractive and repulsive forces to transform a sequence of objective points to a path. Hence, the proposal achieves the task of path planning generation, to solve the limitations given by the original APF in 3D underwater path planning for the AUV, such as the GNRON, U-shaped trap and rotation unreachable. Based on the improved repulsive potential, the GNRON problem is eliminated by adding a coefficient item to the repulsion potential field of obstacles. The attractive potential function can keep away from a U-shaped trap by a rotation matrix F(X). Then, the distance factor function M(X) is considered to improve the attractive potential and solve the rotation unreachable problem caused by the rotation matrix F(X). The pseudo code for the proposed method is shown in Table 1.

Tab. 1. Algorithm of MPF-based velocity synthesis

Input: a means to compute the gradient $\nabla U_{total}(X)$ at X
Output: multipoint sequence $\{X(0), X(1), \cdots, X(i)\}$
1: procedure MPF($\lambda_1, \lambda_2, a, d_o, m, R, O, X$)
2: i=0
3: calculation angle $x, y, z, \theta, \psi, \alpha_1, \alpha_2, \alpha_3$
4: by introducing $\|d_{XG}\|$ and U_{repmax} to improve repulsive potential — GNRON
5: F(X), $B(X) = e^{(-H(X)^m)}$ to improve attractive potential
6: M(X) to further improve attractive potential — rotation unreachable
7: combined velocity vector synthesis method — time-varying current
8: calculate the total potential U_{total}
9: if $\Delta d \leq 0.02m$ —target achieved
10: else i=i+1
the next position for the AUV
11: end if
12: end procedure

Modified repulsive potential for GNRON

When the target is within the influence distance of the obstacle, the global minimum point in the traditional APF method will not be at the target position. This is one of the factors that make the target unreachable. Hence, the distance $\|d_{XG}\|$ is introduced to the repulsive potential as follows:

$$U_{rep}(X) = \begin{cases} 0 & \|d_{XO}\| \geq d_o \\ \frac{1}{2}\lambda_2 \left(\frac{1}{\|d_{XO}\|} - \frac{1}{\|d_o\|}\right)^2 \|d_{XG}\|^a & \|d_{XO}\| < d_o \\ \frac{U_{repmax}}{2(1+\|d_{in}\|^2)} & \|d_{XO}\| < R \end{cases} \quad (8)$$

In view of the above potential, the repulsive force can be expressed as

$$\begin{cases} \vec{F}_{rep}(X) = -\nabla U_{rep}(X) \\ \qquad\qquad = \begin{cases} 0 & \|d_{XO}\| \geq d_o \\ \vec{F}_{rep1}(X) + \vec{F}_{rep2}(X) & \|d_{XO}\| < d_o \\ \vec{F}_{rep3}(X) & \|d_{XO}\| < R \end{cases} \\ |V_{auv}(t)| \sin\alpha_1 = |V_0(t)| \sin(\alpha_2 + \alpha_3) \end{cases} \quad (9)$$

$$\begin{cases} \vec{F}_{rep1}(X) = \lambda_2 \left(\frac{1}{\|d_{XO}\|} - \frac{1}{\|d_o\|}\right) \|d_{XO}\|^{-2} \|d_{XG}\|^a \vec{n}_{OX} \\ \vec{F}_{rep2}(X) = \frac{n}{2}\lambda_2 \left(\frac{1}{\|d_{XO}\|} - \frac{1}{\|d_o\|}\right)^2 \|d_{XG}\|^{a-1} \vec{n}_{XG} \\ \vec{F}_{rep3}(X) = \|d_{in}\| U_{repmax} (1 + \|d_{in}\|)^{-2} \vec{n}_{in} \end{cases} \quad (10)$$

Here, U_{repmax} is the maximum repulsive potential. R is the radius of the obstacle, which is the maximum distance from the centroid to the obstacle. $\vec{n}_{XG}, \vec{n}_{OX}, \vec{n}_{in}$ are the unit vector. $\|d_{in}\|$ is the shortest distance between the obstacle and the AUV. a is a positive parameter.

When moving into the interior of the open obstacle, for example, the following U-shaped obstacles, the maximum repulsive potential is used to ensure obstacle avoidance. The new repulsive potential function can ensure that the total potential has a global minimum at the goal position. So, the AUV can reach the target with the obstacle nearby.

Modified attractive potential for U-shaped trap

When a local minimum point appears within the U-shaped obstacle, the AUV falls into the interior of the U-shaped trap. On the one hand, the maximum repulsive potential is used to ensure obstacle avoidance. On the other hand, to avoid the trap, a rotation matrix F(X) and a strict attenuation function $B(X) = e^{((-H(X)^m))}$ have been introduced. The new attractive potential is defined as follows:

$$U_{att}(X) = \frac{1}{2}\lambda_1 \|d_{XG}\|^2 F(X) \quad (11)$$

Here, θ represents a random angle, and is defined as below:

$$F(X) = \begin{bmatrix} c_\theta & s_\theta & 0 \\ -s_\theta & c_\theta & 0 \\ 0 & 0 & 1 \end{bmatrix} \cdot \begin{bmatrix} c_{(B(X)*\theta)} & -s_{(B(X)*\theta)} & 0 \\ s_{(B(X)*\theta)} & c_{(B(X)*\theta)} & 0 \\ 0 & 0 & 1 \end{bmatrix} \cdot \begin{bmatrix} c_\theta & -s_\theta & 0 \\ s_\theta & c_\theta & 0 \\ 0 & 0 & 1 \end{bmatrix} \quad (12)$$

Among them, $B(X)$ is

$$B(X) = e^{(-H(X)^m)} \quad (13)$$

The attractive force is expressed as follows. It is the negative gradient of the attractive field,

$$\vec{F}_{att}(X) = -\lambda_1 \|d_{XG}\| \vec{n}_{XG} F(X) \quad (14)$$

where s_θ, c_θ are the sine and cosine functions. m is the decay rate. B(X) is a decay function. H(X) is the total force of the MPF. When the magnitude of the total force approaches zero, the value B(X) will be close to one. And as H(X) grows, B(X) will decay rapidly to zero.

If the value B(X) is zero, $\begin{bmatrix} c_{(B(X)*\theta)} & -s_{(B(X)*\theta)} & 0 \\ s_{(B(X)*\theta)} & c_{(B(X)*\theta)} & 0 \\ 0 & 0 & 1 \end{bmatrix}$ and F(X) are the identity matrices. Similarly, the direction of the total force will not be rotated. When the value of B(X) is one, the rotation matrix is as follows:

$$F(X) = \begin{bmatrix} c_\theta & -s_\theta & 0 \\ s_\theta & c_\theta & 0 \\ 0 & 0 & 1 \end{bmatrix}$$

Based on this, the direction of the total force will rotate degrees. After that, the AUV will escape the U-shaped trap. However, the rotation matrix will make the AUV rotate around the target when approaching the target. Hence, the AUV cannot reach the target, which is called rotation unreachable (a special case of GNRON and U-shaped trap).

A further modified attractive potential for rotation unreachable

As noted earlier, the modified attractive potential makes the AUV avoid the U-shaped trap problem effectively by introducing the rotation matrix. However, it will cause rotation unreachable.

According to (8) and (14), when the AUV approaches the target, the total force will gradually decrease. When the total force decays to a non-zero value, the situation of rotation unreachable will occur. In this situation, the AUV will rotate around the target. In order to solve the above problem, a distance factor function M(X) is introduced:

$$M(X) = \frac{1}{\|d_{XG}^2\|} + 1 \quad (15)$$

The further modified attractive force is

$$\begin{cases} \vec{F}_{att}(X) = -\lambda_1 \|d_{XG}\| \vec{n}_{XG} F(X) M(X) \\ |V_{auv}(t)| \sin\alpha_1 = |V_c(t)| \sin(\alpha_2 + \alpha_3) \end{cases} \quad (16)$$

As the AUV moves away from the target, M(X) is approximately equal to one. When the AUV approaches the target, its growth rate is greater than the decay rate of $\|d_{XG}\|$. Hence, as the AUV approaches the target, the magnitude of the attractive force will increase rapidly. Since F(X) is an identity matrix, the attractive force will not rotate. The further modified attractive potential can avoid rotation unreachable.

Combining the velocity vector synthesis method (7) and MPF (9)(10)(16), the proposed algorithm can realize 3D underwater path planning with time-varying and static obstacles. In summary, both the attractive and repulsive potential have been modified, and this overcomes the limitation of the traditional APF.

SIMULATIONS AND ANALYSIS

Considering that this work aims to achieve 3D underwater path planning for an AUV with time-varying current and static obstacles, and the MPF-based velocity synthesis method is applied to effectively solve the limitations of the APF and ocean current, three simulation conditions were carefully selected. The starting point was set at $X = (0,0,0)^T$ and the target point at $G = (20,20,15)^T$. According to Assumptions 1-3, the simulation experiments are as follows to accomplish comparisons of the proposed method concerning traditional APF. Besides, the time-varying ocean current is described as follows [39]:

$$\varphi(x,y,t) = 1 - \tanh\left(\frac{y - B(t)\cos(k(x-ct))}{\left(1+\gamma^2 B(t)^2 \sin^2\left((k(x-ct))\right)\right)^{0.5}}\right) \quad (17)$$

$$B(t) = B_0 + \delta\cos(\omega_0 t + \phi) \quad (18)$$

where $\left(-\frac{\partial\varphi}{\partial y}, \frac{\partial\varphi}{\partial x}\right)$ is the velocity of the ocean current, and the parameters are set as $c = 0.15$, $k = 1$, $\gamma = 0.88$, $B_0 = 0.15$ $\delta = 0.3$, $\omega_0 = 0.4$.

Meanwhile, it is assumed that the AUV is moving at a constant speed, and the total force applied to it only determines the direction of its motion. Then, if the distance from the AUV to the target is less than 0.02 m, it indicates that the AUV has reached the target. First, the design parameters of the best planning effect are selected by using the APF method through simulation results. In the simulation, the AUV must not only avoid obstacles but also overcome the influence of time-varying current, and the VS algorithm was introduced to overcome the influence of the current by adjusting the navigation direction of the AUV. Afterward, the same parameters for the APF and MPF-based VS are used to make comparisons for each situation. In the following simulation, the blue circle represents part of the AUV location.

A. Simulation comparison for GNRON

When the target is close to an obstacle, it will cause the GNRON problem in Fig. 6. Both the traditional APF and the MPF-based VS method are compared to confirm the effectiveness of the improvement. For this test, the APF parameters are $\lambda_1 = 2$, $\lambda_2 = 3$, $d_o = 3$, $m = 2$, $R = 0.5$. The parameters of the MPF-based VS are $\lambda_1 = 2$, $\lambda_2 = 3$, $a = 0.5$, $d_o = 3$, $m = 2$, $R = 0.5$. There is an obstacle with the coordinate of $O = (19.5,19.5,14)^T$. In Fig. 7, the modified repulsive potential is adopted. It can be concluded from the above simulation that both the potentials can ensure that the AUV reaches the target point while avoiding obstacles. But when the AUV approaches the target, it will oscillate due to obstacles near the target. After the repulsive potential is modified by $\|d_{XG}\|$, it rapidly decreases near the target, and the AUV finally reaches the target.

B. Simulation comparison for U-shaped trap

Fig. 8 and Fig. 9 show a U-shaped trap simulation test, which is the best-known problematic situation in the traditional APF. In this situation, a rotation matrix and a strict attenuation function are chosen to improve the attractive potential. The APF parameters are $\lambda_1 = 0.01$, $\lambda_2 = 5$, $d_o = 5$, $m = 2$, $R = 1$; the parameters of the MPF-based VS are $\lambda_1 = 2$, $\lambda_2 = 3$, $a = 0.5$, $d_o = 3$, $m = 2$, $R = 1$. The obstacle position is $O = (10,10,7.5)^T$. Obviously, it will sink into the U-shaped trap by the traditional APF, and the maximum repulsive potential is used to avoid the collision obstacle in Fig. 8. Fig. 9 shows the path generated by the proposed method, and the AUV reaches the target away from the trap. From the above simulation results, it is shown that the proposed MPF-based VS method can make the AUV rotate and avoid dropping into the U-shaped trap efficiently.

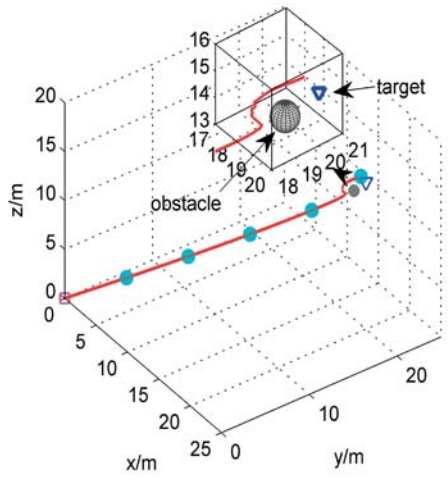

Fig. 6. Simulation of traditional repulsive potential

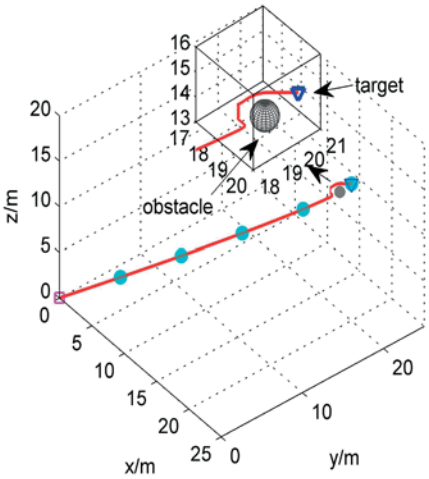

Fig. 7. Simulation of modified repulsive potential

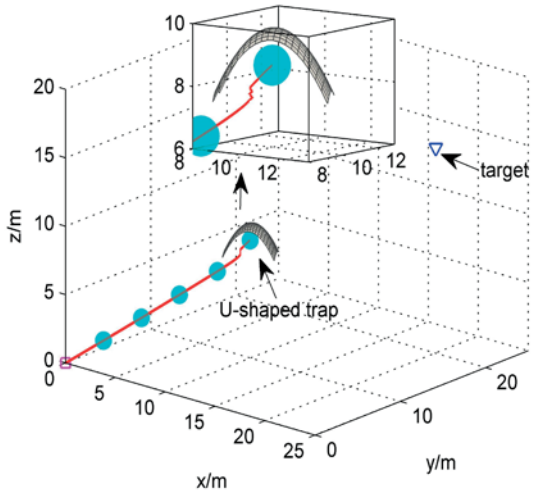

Fig. 8. Simulation of the traditional APF

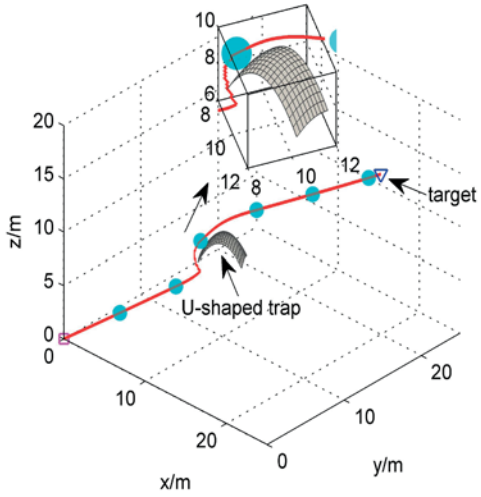

Fig. 9. Simulation of the MPF-based VS

C. Simulation comparison for rotation unreachable

When the modified attractive function is introduced, the rotation unreachable may be generated, as shown in Fig. 10. For this part, the parameters are $\lambda_1 = 2.8$, $\lambda_2 = 2.8$, $a = 1.5$, $d_o = 6$, $m = 2$. The obstacle position is as follows:

R=[0.5;1.5;1.2;1.2;1.5;1.5;1.2;1.5;1.5;1.5;1.5],

$$0 = \begin{bmatrix} 3,2.5,2;\ 4.5,4.5,2.5;\ 3,6,4;\ 6,2,5;\ 6,2,5;\ 7.5,9,6;\ 9,6,7; \\ 14,8,6;\ 14.5,16,10;\ 16,12,10;\ 18,18,12;\ 20,16,6 \end{bmatrix}^T$$

Fig. 10 represents the problem of rotation unreachable by a rotation matrix F(X). When the AUV approaches the target, it starts to rotate around the target. As shown in Fig. 11, under the action of the modified repulsive potential and further modified attractive potential, the AUV can reach the target point while avoiding obstacles.

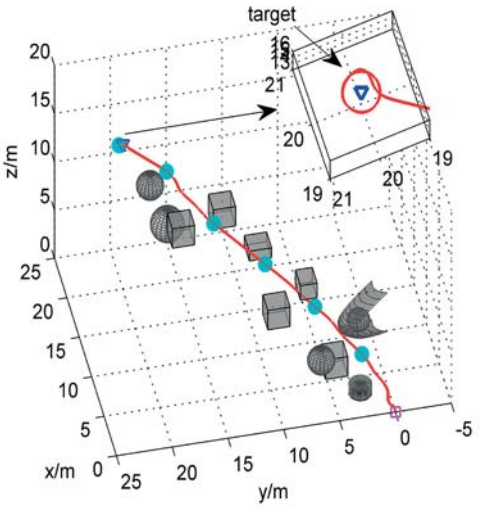

Fig. 10. Rotation unreachable caused by new attractive function

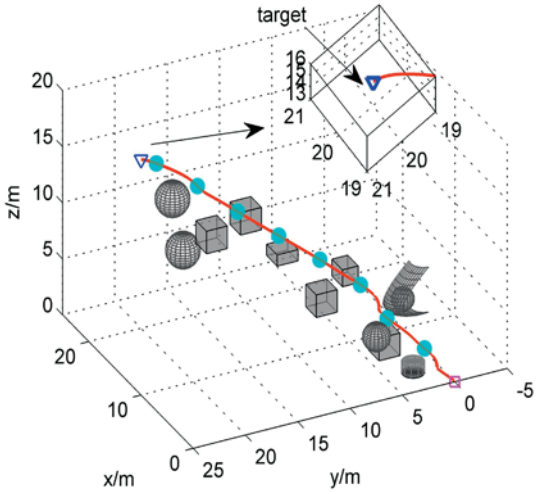

Fig. 11. Simulation of the MPF-based VS

In summary, the proposed algorithm has been effectively tested for an AUV under time-varying current and different static obstacles environments. The theoretical analysis and simulation comparison results above prove that 3D underwater path planning using the proposed MPF-based VS method can get better performance than the traditional APF method. Meanwhile, the 3D path planning simulation results of the AUV prove that the proposed method can effectively deal with the GNRON, U-shaped trap, and rotation unreachable problems under a variety of static obstacles environments.

CONCLUSION

In this article, 3D path planning in environments with time-varying current and static obstacles is studied for an AUV and a novel MPF-based velocity synthesis method is proposed. This proposed method has a concise mathematical description

and algorithm structure, and has solved the problems of the traditional APF, such as the GNRON, U-shaped trap, and rotation unreachable. To offset the influence of the current, the VS method is designed to adjust the moving direction of the AUV. Besides, based on the multi-beam FLS model, it is suitable for path planning in a complex underwater environment. Finally, the simulation results show the good performance of this algorithm. For future work, the energy consumption will be considered in the path planning of AUVs.

ACKNOWLEDGEMENTS

This work was supported by the National Natural Science Foundation of China (52101298, 52201409), the China Postdoctoral Science Foundation (2019M661082), and the Fundamental Research Funds for the Central Universities (3132022104, 3132021107, 3132019319).

REFERENCES

1. T. Yan, Z. Xu, S. X. Yang, and S. A. Gadsden, "Formation Control of Multiple Autonomous Underwater Vehicles: a review," *Intelligence & Robotics*, vol. 3, no. 1, 2023, doi: 10.20517/ir.2023.01.

2. H. Choukri and L. Z. Qidan, "Path Following Control of Fully Actuated Autonomous Underwater Vehicle Based on LADRC," *Polish Maritime Research*, vol. 25, no. 4, 2018, doi: 10.2478/pomr-2018-0130.

3. W. Yu, K. H. Low, and L. Chen, "Cooperative Path Planning for Heterogeneous Unmanned Vehicles in a Search-and-Track Mission Aiming at an Underwater Target," *IEEE Trans. Veh. Technol.*, vol. 99, 2020, doi:10.1109/TVT.2020.2991983.

4. L. Rowinski and M. Kaczmarczyk, "Evaluation of Effectiveness of Water-jet Propulsor for a Small Underwater Vehicle," *Polish Maritime Research*, vol. 28, no. 4, 2022, doi: 10.2478/pomr-2021-0047.

5. S. Wang, H. Zhang, S. Baldi, and R. Zhong, "Leaderless Consensus of Heterogeneous Multiple Euler-Lagrange Systems with Unknown Disturbance," *ArXiv*, 2021, doi:10.1109/tac.2022.3172594.

6. S. Wang and X. Meng, "Adaptive Consensus and Parameter Estimation of Multi-agent Systems with an Uncertain Leader," *IEEE Trans. Autom. Control*, vol. 66, 2020, doi:10.1109/tac.2020.3046215.

7. S. Wang, H. Zhang, and Z. Chen, "Adaptive Cooperative Tracking and Parameter Estimation of an Uncertain Leader over General Directed Graphs," *IEEE Trans. Autom. Control*, 2020, doi:10.1109/tac.2022.3197670.

8. Z. Zeng, L. Lian, K. Sammut, F. He, Y. Tang, and A. Lammas, "A Survey on Path Planning for Persistent Autonomy of Autonomous Underwater Vehicles," *Ocean Engineering*, vol. 110, 2015, doi:10.1016/j.oceaneng.2015.10.007.

9. Y. Ma, Y. Gong, C. Xiao, Y. Gao, and J. Zhang, "Path Planning for Autonomous Underwater Vehicles: An Ant Colony Algorithm Incorporating Alarm Pheromone," *IEEE Trans. Veh. Technol.*, 2018, doi:10.1109/TVT.2018.2882130.

10. B. Hadi, A. Khosravi, and P. Sarhadi, "A Review of the Path Planning and Formation Control for Multiple Autonomous Underwater Vehicles," *Journal of Intelligent & Robotic Systems*, vol. 101, no. 4, 2021, doi:10.1007/s10846-021-01330-4.

11. L. Song, H. Chen, W. Xiong, Z. Dong, P. Mao, Z. Xiang, and K. Hu, "Method of Emergency Collision Avoidance for Unmanned Surface Vehicle (USV) Based on Motion Ability Database," *Polish Maritime Research*, vol. 26, no. 2, 2019, doi: 10.2478/pomr-2019-0025.

12. N. Lefebvre, I. Schjølberg, and I. Utne, "Integration of Risk in Hierarchical Path Planning of Underwater Vehicles," *IFAC PapersOnLine*, vol. 49, no. 23, 2016, doi:10.1016/j.ifacol.2016.10.347.

13. Z. Zeng, K. Sammut, L. Lian, F. He, A. Lammas, and Y. Tang, "A Comparison of Optimization Techniques for AUV Path Planning in Environments with Ocean Currents," *Robotics and Autonomous Systems*, vol. 82, 2016, doi: 10.1016/j.robot.2016.03.011.

14. H. Niu, Y. Lu, A. Savvaris, and A. Tsourdos, "An Energy-Efficient Path Planning Algorithm for Unmanned Surface Vehicles," *Ocean Engineering*, vol. 161, 2018, doi: 10.1016/j.oceaneng.2018.01.025.

15. Y. Li, F. Zhang, D. Xu, and J. Dai, "Liveness-Based RRT Algorithm for Autonomous Underwater Vehicles Motion Planning," *Journal of Advanced Transportation*, 2017, doi: 10.1155/2017/7816263.

16. R. Cui, L. Yang, and W. Yan, "Mutual Information-Based Multi-AUV Path Planning for Scalar Field Sampling Using Multidimensional RRT," *IEEE Trans. Syst., Man, Cybern.: Syst.*, vol. 46, no. 7, 2017, doi: 10.1109/TSMC.2015.2500027.

17. K. Sun and X. Liu, "Path Planning for an Autonomous Underwater Vehicle in a Cluttered Underwater Environment Based on the Heat Method," *International Journal of Applied Mathematics and Computer Science*, vol. 31, 2021, doi: 10.34768/amcs-2021-0020.

18. R. Song, Y. Liu, and R. Bucknall, "A Multi-Layered Fast Marching Method for Unmanned Surface Vehicle Path Planning in a Time-variant Maritime Environment,"

Ocean Engineering, vol. 129, 2017, doi: 10.1016/j.oceaneng.2016.11.009.

19. Y. K. Hwang and N. Ahuja, "A Potential Field Approach to Path Planning," *IEEE Trans. Robot. Autom.*, vol. 8, no. 1, 1992, doi: 10.1109/70.127236.

20. S. Saravankumar and T. Asokan, "Multipoint Potential Field Method for Path Planning of Autonomous Underwater Vehicles in 3D Space," *Intelligent Service Robotics*, vol. 6, no. 4, 2013, doi: 10.1007/s11370-013-0138-2.

21. S. S. Ge and Y. J. Cui, "New Potential Functions for Mobile Robot Path Planning," *IEEE Trans. Robot. Autom.*, vol. 16, no. 5, 2000, doi:10.1109/70.880813.

22. E. Hernandez, M. Carreras, and P. Ridao, "A Comparison of Homotopic Path Planning Algorithms for Robotic Applications," *Robotics & Autonomous Systems*, vol. 64, 2015, doi: 10.1016/j.robot.2014.10.021.

23. S. Wang, M. Fu, Y. Wang, and L. Zhao, "A Multi-Layered Potential Field Method For Water-Jet Propelled Unmanned Surface Vehicle Local Path Planning With Minimum Energy Consumption," *Polish Maritime Research*, vol. 26, no. 1, 2019, doi: 10.2478/pomr-2019-0015.

24. J. Song, C. Hao, and J. Su, "Path Planning for Unmanned Surface Vehicle Based on Predictive Artificial Potential Field," *International Journal of Advanced Robotic Systems*, vol. 17, 2020, doi: 10.1177/1729881420918461.

25. M. Fu, S. Wang, and Y. Wang, "Multi-Behavior Fusion Based Potential Field Method for Path Planning of Unmanned Surface Vessel," *China Ocean Engineering*, vol. 33, no. 5, 2019, doi: 10.1007/s13344-019-0056-y.

26. Y. Rasekhipour, A. Khajepour, Shih-Ken Chen, and B. Litkouhi, "A Potential Field-Based Model Predictive Path-Planning Controller for Autonomous Road Vehicles," *IEEE Trans. Intell. Transp. Syst.*, vol. 18, no. 5, 2017, doi: 10.1109/TITS.2016.2604240.

27. Y. Huang, H. Ding, Y. Zhang, H. Wang, D. Cao, N. Xu, and C. Hu, "A Motion Planning and Tracking Framework for Autonomous Vehicles Based on Artificial Potential Field-Elaborated Resistance Network (APFE-RN) Approach," *IEEE Trans. Ind. Electron.*, vol. 67, no. 2, 2019, doi: 10.1109/TIE.2019.2898599.

28. J. Lee, "Heterogeneous-ants-based Path Planner for Global Path Planning of Mobile Robot Applications," *International Journal of Control Automation & Systems*, vol. 15, no. 5, 2017, doi: 10.1007/s12555-016-0443-6.

29. Y. Sun, X. Luo, X. Ran, and G. Zhang, "A 2D Optimal Path Planning Algorithm for Autonomous Underwater Vehicle Driving in Unknown Underwater Canyons," *Journal of Marine Science and Engineering*, vol. 9, no. 3, 2021, doi: 10.3390/jmse9030252.

30. E. Vidal, J. D. Hernández, K. Istenič, and M. Carreras, "Online View Planning for Inspecting Unexplored Underwater Structures," *IEEE Robot. Autom. Lett.*, vol. 2, no. 3, 2017, doi: 10.1109/LRA.2017.2671415.

31. D. Zhu, W. Li, M. Yan, and Simon X. Yang, "The Path Planning of AUV Based on D-S Information Fusion Map Building and Bio-Inspired Neural Network in Unknown Dynamic Environment," *International Journal of Advanced Robotic Systems*, vol. 11, no. 3, 2014, doi: 10.5772/56346.

32. X. Yao, F. Wang, C. Yuan, J. Wang, and X. Wang, "Path Planning for Autonomous Underwater Vehicles based on Interval Optimization in Uncertain Flow Fields," *Ocean Engineering*, vol. 234, 2021, doi: 10.1016/j.oceaneng.2021.108675.

33. D. Zhu, H. Huang, and S. X. Yang, "Dynamic Task Assignment and Path Planning of Multi-AUV System Based on an Improved Self-Organizing Map and Velocity Synthesis Method in Three-Dimensional Underwater Workspace," *IEEE Trans. Cybern.*, vol. 43, no. 2, 2013, doi: 10.1109/TSMCB.2012.2210212.

34. Y. Li, T. Ma, P. Chen, Y. Jiang, R. Wang, and Q. Zhang, "Autonomous Underwater Vehicle Optimal Path Planning Method for Seabed Terrain Matching Navigation," *Ocean Engineering*, vol. 133, 2017, doi: 10.1016/j.oceaneng.2017.01.026.

35. B. Sun, D. Zhu, and S. X. Yang, "An Optimized Fuzzy Control Algorithm for Three-Dimensional AUV Path Planning," *International Journal of Fuzzy Systems*, vol. 20, no. 2, 2018, doi: 10.1007/s40815-017-0403-1.

36. H. N. Esfahani and R. Szlapczynski, "Model Predictive Super-Twisting Sliding Mode Control for an Autonomous Surface Vehicle," *Polish Maritime Research*, vol. 26, no. 3, 2019, doi: 10.2478/pomr-2019-0057.

37. Z. Dong, Y. Liu, H. Wang, and T. Qin, "Method of cooperative formation control for underactuated USVS based on nonlinear backstepping and cascade system theory," *Polish Maritime Research*, vol. 28, no. 1, 2021, doi: 10.2478/pomr-2021-0014.

38. C. Lin, H. Wang, J. Yuan, and M. Fu, "An Online Path Planning Method Based on Hybrid Quantum Ant Colony Optimization for AUV," *International Journal of Robotics & Automation*, vol. 106, 2018, doi: 10.2316/Journal.206.2018.4.206-5337.

39. M. Chen and D. Zhu, "Optimal Time-Consuming Path Planning for Autonomous Underwater Vehicles Based on a Dynamic Neural Network Model in Ocean Current Environments," *IEEE Trans. Veh. Technol.*, vol. 69, no. 12, 2020, doi: 10.1109/TVT.2020.3034628.